Chemistry & Biology
Article

Anamorsin Is a [2Fe-2S] Cluster-Containing Substrate of the Mia40-Dependent Mitochondrial Protein Trapping Machinery

Lucia Banci,[1,2,*] Ivano Bertini,[1,2,*] Simone Ciofi-Baffoni,[1,2] Francesca Boscaro,[3] Afroditi Chatzi,[4,5] Maciej Mikolajczyk,[1,2] Kostas Tokatlidis,[4,6] and Julia Winkelmann[1,2]
[1]Magnetic Resonance Center CERM, University of Florence, Via L. Sacconi 6, 50019, Sesto Fiorentino, Florence, Italy
[2]Department of Chemistry, University of Florence, Via della Lastruccia 3, 50019 Sesto Fiorentino, Florence, Italy
[3]Centro Interdipartimentale di Spettrometria di Massa (CISM), University of Florence, Viale G. Pieraccini 6, 50139 Florence, Italy
[4]Institute of Molecular Biology and Biotechnology, Foundation for Research and Technology Hellas (IMBB-FORTH), Heraklion, 70013 Crete, Greece
[5]Department of Biology, University of Crete, Heraklion, 71409 Crete, Greece
[6]Department of Materials Science and Technology, University of Crete, Heraklion, 71003 Crete, Greece
*Correspondence: banci@cerm.unifi.it (L.B.), bertini@cerm.unifi.it (I.B.)
DOI 10.1016/j.chembiol.2011.03.015

SUMMARY

Human anamorsin was implicated in cytosolic iron-sulfur (Fe/S) protein biogenesis. Here, the structural and metal-binding properties of anamorsin and its interaction with Mia40, a well-known oxidoreductase involved in protein trapping in the mitochondrial intermembrane space (IMS), were characterized. We show that (1), anamorsin contains two structurally independent domains connected by an unfolded linker; (2), the C-terminal domain binds a [2Fe-2S] cluster through a previously unknown cysteine binding motif in Fe/S proteins; (3), Mia40 specifically introduces two disulfide bonds in a twin CX_2C motif of the C-terminal domain; (4), anamorsin and Mia40 interact through an intermolecular disulfide-bonded intermediate; and (5), anamorsin is imported into mitochondria. Hence, anamorsin is the first identified Fe/S protein imported into the IMS, raising the possibility that it plays a role in cytosolic Fe/S cluster biogenesis also once trapped in the IMS.

INTRODUCTION

Besides their well-established function in energy supply for all cell compartments, mitochondria are also the primary source of iron-sulfur (Fe/S) clusters that are utilized by proteins throughout the cell. Such Fe/S cluster proteins have essential functions in metabolism, electron transfer, and regulation of gene expression. Despite the relative simplicity of Fe/S clusters in terms of structure and composition (Andreini et al., 2009; Bertini et al., 1995), their synthesis and assembly is a highly complex and coordinated process that has not yet been completely understood (Lill, 2009).

The Fe/S cluster biogenesis in eukaryotes involves three distinct machineries localized in two different cellular compartments: (1), the iron-sulfur cluster (ISC) assembly machinery; (2), the ISC export machinery, both in mitochondria; and (3), the cytosolic iron-sulfur cluster assembly (CIA) machinery in the cytoplasm (Lill and Mühlenhoff, 2008), which requires components of the mitochondrial machineries to allow the formation of the extra-mitochondrial Fe/S clusters. Generation of extra-mitochondrial (both cytosolic and nuclear) Fe/S proteins requires a yet unidentified product, produced by the ISC assembly pathway and exported to the cytosol by the ISC export machinery. Even if it became clear that the ISC and CIA components of higher eukaryotes studied so far perform similar, if not identical, roles as in yeast, several of human ISC assembly proteins have been detected, at variance with yeast homologs, in a low amount in the cytosol and/or nucleus of human cells (Rouault and Tong, 2005; Tong et al., 2003; Tong and Rouault, 2006).

In yeast, the protein Dre2 has been suggested to be implicated in the cytosolic Fe/S protein maturation (Zhang et al., 2008). Dre2 is a Fe/S cluster protein and either depletion or mutations of *dre2* result in phenotypes similar to those caused by alteration of CIA components. Additionally, it has been found recently that the diflavin reductase Tah18, which is also part of the yeast CIA machinery, forms a complex with Dre2 in the cytosol (Netz et al., 2010). This complex is part of an electron transfer chain functioning in an early step of the cytosolic Fe/S protein biogenesis (Netz et al., 2010). The pathway is conserved in mammals as the human counterparts can functionally replace the yeast Tah18 and Dre2 proteins in yeast (Netz et al., 2010) and the human Dre2 homolog can restore viability of a *Δdre2* deletion *Saccharomyces cerevisiae* strain (Zhang et al., 2008). However, in sharp difference to all other CIA protein components, for which no mitochondrial localization has ever been reported, a fraction of Dre2 is localized in the mitochondrial IMS (Zhang et al., 2008). Additionally, it has been reported that Tah18 relocalizes to mitochondria on high oxidative stress levels thereby acting as a molecular stress-sensor and controls mitochondria-mediated oxidative-induced cell death pathway in yeast (Vernis et al., 2009). How the dual mitochondrial/cytoplasmic localization of Dre2 and Tah18 is accomplished is still unknown. Because Dre2 has two CX_2C motifs, similar to some other IMS proteins, it has been proposed (Zhang et al., 2008) that the

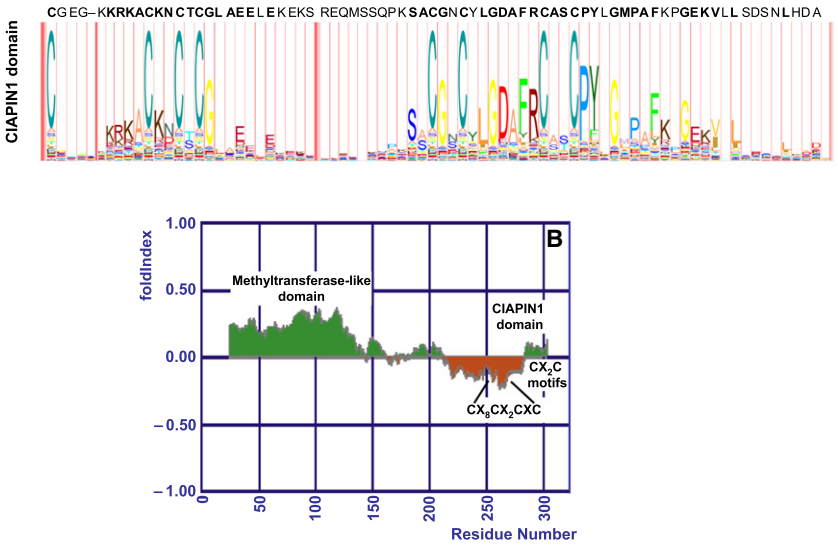

Figure 1. Bioinformatic Analysis of Anamorsin

(A) Sequence alignment of the CIAPIN1 domain conserved in 182 sequences by using LogoMat-M visualization tool (Schuster-Böckler et al., 2004). The relative size of a letter expresses its probability to occur at this position in the sequence alignment. Pink column indicates an insert region of a number of residues with no conservation in the sequence alignment.

(B) Folding prediction of anamorsin derived from FoldIndex program (Prilusky et al., 2005). Regions shaded in green are predicted to be in a folded state, whereas red-shaded regions are predicted to be unfolded.

dual cellular protein distribution might involve an oxidative trapping mechanism in the IMS performed by the oxidoreductase Mia40 and the sulfhydryl oxidase Erv1 (named ALR in human). The latter proteins trap a class of mitochondrial proteins in the IMS having characteristic cysteine motifs (twin CX_3C, CX_9C, or CX_2C) (Gabriel et al., 2007; Sideris et al., 2009).

Besides being associated with Fe/S cluster biogenesis (Netz et al., 2010; Zhang et al., 2008), the human homolog of Dre2, called anamorsin or ciapin1, has also been identified as a necessary molecule for the antiapoptotic effects of various cytokines in hematopoiesis (Shibayama et al., 2004). Additionally, anamorsin was reported to be involved in the development of multidrug resistance in leukemia cells (Hao et al., 2006a) and to be associated with increased tumor recurrence, making anti-anamorsin therapy a new cancer treatment strategy (Li et al., 2010).

In this work, the structural characterization and metal binding properties of anamorsin, and indirectly of Dre2, have been obtained. To contribute to the comprehension of the functional role of anamorsin, we have investigated its interaction with Mia40 and its import into isolated yeast mitochondria. From this analysis we conclude that (1), anamorsin is a Mia40-dependent but ALR-independent IMS-protein; and (2), it can bind a [2Fe-2S] cluster before and after specific Mia40-driven Cys-oxidation. Hence, anamorsin is the first identified Fe/S cluster protein imported into the IMS, raising the possibility that anamorsin plays a role in cytosolic Fe/S cluster biogenesis also once trapped in the IMS.

RESULTS

Anamorsin Has a CIAPIN1 Domain Potentially Responsible of Its IMS Trapping through the Mitochondrial Mia40-ALR Machinery

Bioinformatic analysis (see Supplemental Experimental Procedures available online) shows that a CIAPIN1 domain is present in the anamorsin amino acid sequence. The CIAPIN1 domain contains a highly conserved cysteine pattern, i.e., $\mathbf{CX_{5\text{-}14}CX_2CXCX_nCX_2CX_7CX_2C}$ (Figure 1A), and is present in 182 sequences found in 103 eukaryotic species (average length of the domain 85 aa). The CIAPIN1 domain is typically located at the C terminus and can be fused to other functional domains. In both anamorsin and Dre2, the CIAPIN1 domain is fused at the N terminus to a methyltransferase-like domain. Secondary structure and folding predictions reveal that these two domains in anamorsin are separated by an unstructured amino acid linker of ~50 residues (Figure 1B) and that a large part of the CIAPIN1 domain, in particular its initial segment (residues 222–266), is structurally highly disordered, whereas the final segment is predicted to be more structured (Figure 1B). The latter region of the CIAPIN1 domain contains a twin CX_2C motif whereas the initial segment of the CIAPIN1 domain contains the four additional cysteines of the highly conserved cysteine pattern (Figure 1B). Because it has been shown that the homologous yeast protein Dre2 can bind a Fe/S cofactor (Zhang et al., 2008), it is likely that cysteines of the highly conserved cysteine pattern in anamorsin are involved in iron binding.

Anamorsin Contains a Well-Folded N-Terminal Domain and a Largely Unstructured, Flexible C-Terminal Part Carrying an Iron Center

Recombinant expression of anamorsin in the presence of iron and subsequent purification (Supplemental Experimental Procedures) results in a reddish-brown protein solution suggesting the presence of an iron metal center. The protein is monomeric in solution and gets degraded within 7–10 days at room temperature under anaerobic conditions resulting to yield a stable fragment of 19 kDa (Figure 2). Mass spectrometry analysis (Supplemental Experimental Procedures) revealed that the stable fragment is constituted by the N-terminal part spanning aa 1–172 of the protein. During degradation, the color of the anamorsin solution is lost, indicating that iron is released. Because the remaining stable fragment does not contain cysteines of the CIAPIN1 domain, at least one of the latter cysteines is essential for iron binding.

The ^{1}H-^{15}N HSQC spectra of the full-length protein (Figure 2A) shows highly crowded cross-peaks in the spectral region between 8 and 8.5 ppm indicating that the protein contains an unstructured region, in addition to several signals spread over a larger spectral range, indicative of folded conformations.

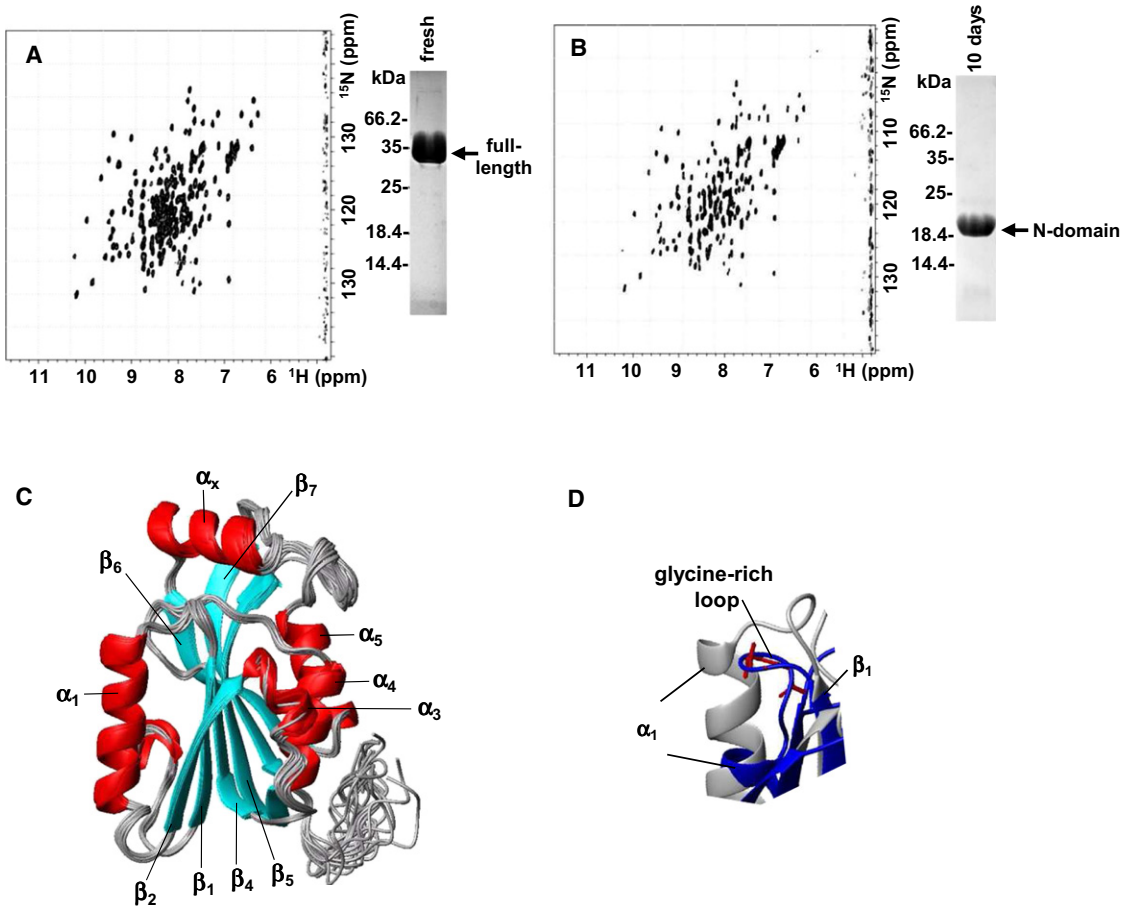

Figure 2. Structural Properties of Anamorsin

(A and B) ^{1}H-^{15}N HSQC spectrum at 500 MHz and 308 K of (A) a freshly purified [2Fe-2S]-anamorsin and (B) of anamorsin after 10 days of incubation under anaerobic conditions. SDS PAGE of the corresponding samples (see also Figure S1).

(C) Ribbon representation of the 20 conformers with the lowest energy (see also Table S1). The numbering of the secondary structure elements is according to a typical SAM-dependent methyltransferase fold (α_x: α-helix insertion in the N-terminal domain of anamorsin).

(D) Section of the overlay between the structures of the N-terminal domain of anamorsin (gray) and the structurally closest methyltransferase (blue, BH2331 of *Bacillus halodurans*, glycine residues are in red).

After degradation, the ^{1}H-^{15}N HSQC spectrum of the resulting fragment (Figure 2B) shows the disappearance of many of the signals in the crowded, central region, whereas the well-resolved resonances are still present and do not show significant chemical shift changes. ^{15}N{^{1}H} NOEs experiments on the full-length anamorsin showed that the residues not belonging to the N-terminal domain (that are all in the highly crowded spectral region between 8 and 8.5 ppm) exhibited negative or very low NOEs, indicative of a high degree of flexibility in the C-terminal part of the protein (Figure S1). We can conclude that the N-terminal part is well-folded whereas the C-terminal part, comprising both the linker and CIAPIN1 domain, is largely unstructured and flexible and therefore, highly prone to degradation.

The solution structure of the well-folded N-terminal domain (aa 1–172) was solved by nuclear magnetic resonance (NMR) (Supplemental Experimental Procedures and Table S1). It shows the presence of five α-helical and six β strand alternated structural elements (Figure 2C). The β strands are all parallel, except for the last that is antiparallel. They form a sheet around which the α helices are arranged (Figure 2C). This fold resembles the core fold of S-adenosyl-L-methionine (SAM)-dependent methyltransferases. The order of the β strands in these proteins is generally 3214576 that is also found in the N-terminal domain of anamorsin with the exception that the third β strand is absent. In addition, the fold of anamorsin diverges from SAM-dependent methyltransferases in the lack of the second α-helix and in the insertion of an α-helix between the two last β strands (helix α_x). The glycine-rich motif in the loop between the first β strand and first α-helix, which is typically responsible for the binding of the cofactor SAM in such methyltransferases (Kagan and Clarke, 1994; Martin and McMillan, 2002; Schluckebier et al., 1995) is not conserved in the N-terminal domain of anamorsin (Figure 2D). These structural differences suggest that the N-terminal domain of anamorsin is not involved in SAM-binding. This is verified by incubating the ^{15}N-labeled N-terminal domain with a large excess of SAM molecule and then performing ^{1}H-^{15}N HSQC experiments, which showed no chemical shift differences

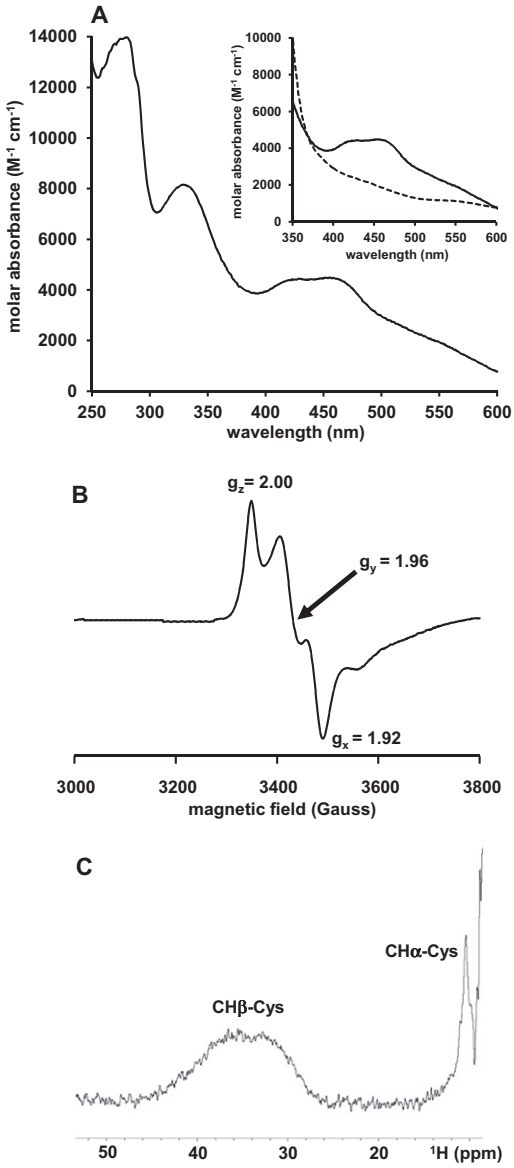

Figure 3. Anamorsin Binds a [2Fe-2S] Cluster

(A) UV-visible spectrum of [2Fe-2S]-anamorsin in 50 mM phosphate buffer, pH 7.0. In the inset, UV-visible spectra of anamorsin without (solid line) or with 1 mM sodium dithionite (dashed line) are shown.

(B) Electron paramagnetic resonance (EPR) spectrum of [2Fe-2S]-anamorsin (200 μM) in 50 mM Tris-HCl pH 8.0, 500 mM NaCl, and 10% glycerol in the presence of 1 mM dithionite at 45 K.

(C) Paramagnetic ^{1}H NMR spectrum of [2Fe-2S]-anamorsin (2 mM) in 50 mM phosphate buffer pH 7.0 at 600 MHz and 298 K (see also Figure S2).

before and after SAM addition. Therefore, this domain is probably rather involved in partner recognition.

Comparison of the signals that can be unambiguously assigned in both, the full-length and the N-terminal domain ^{1}H-^{15}N HSQC spectra (70 spread over the entire sequence), shows similar chemical shifts with average weighted Δ_{HN} values being smaller than 0.05 ppm (Figure S1) (except for two residues at the beginning and the last residues of the N-terminal domain). This result indicates that there are no interactions between the N- and C-terminal domains in the full-length protein; therefore the cysteines involved in iron coordination are all part of the CIAPIN1 domain, because the cysteine(s) of the highly conserved cysteine pattern are necessary for iron binding.

Anamorsin Coordinates a [2Fe-2S] Cluster in the CIAPIN1 Domain

The binding motifs for the different Fe/S clusters in proteins are not highly conserved, yet some consensus motifs have been recognized (Andreini et al., 2007; Lill and Mühlenhoff, 2008). In particular, the binding motifs for the different [2Fe-2S] cluster proteins are classified into three main groups (Andreini et al., 2009; Bertini et al., 2002). However, comparison of the anamorsin cysteine motifs with these groups gave no clear hint on the kind of cluster.

Chemical reconstitution of full-length anamorsin with a 10-fold excess of iron and sulfur in the presence of DTT (Supplemental Experimental Procedures) resulted in an enhanced intensity of its reddish-brown color. At a protein concentration of 76 μM the amount of iron and sulfur was determined to be 150 μM and 157 μM, respectively (Supplemental Experimental Procedures). Such Fe/S/protein ratio of 2:2:1 obtained after cluster reconstitution has been achieved in all preparations.

In the ultraviolet/visible (UV/vis) spectra (Figure 3A) an absorption peak at 333 nm and weaker, broad peaks at ~420 nm and 460 nm are observed, that are typical absorption features of [2Fe-2S] clusters (Morimoto et al., 2002). These absorbances are quenched after reduction of the cluster with 1 mM dithionite (Figure 3A, inset). The protein with the oxidized cluster is electron paramagnetic resonance (EPR) silent consistent with the presence of a S = 0 $[2Fe\text{-}2S]^{2+}$ cluster. Anaerobic addition of dithionite results in cluster reduction and the resulting spectra measured at 45 K (Figure 3B) exhibits a rhombic pattern with g values of g_z 2.00, g_y 1.96, and g_x 1.92, consistent with a S = 1/2 $[2Fe\text{-}2S]^{+}$ cluster. The shape and the g-values are similar to those of plant-like ferredoxins (Palmer and Sands, 1966) and identical g-values have been reported for the yeast homolog Dre2 under these conditions (Zhang et al., 2008). The 600 MHz ^{1}H paramagnetic NMR spectrum (Figure 3C) of the oxidized protein at 298 K shows a broad peak around 34 ppm (CH_{β}-Cys protons) and a sharp signal at 10.5 ppm (CH_{α}-Cys protons). These signals are typical of proteins with an oxidized [2Fe-2S] cluster (Banci et al., 1990; Bertini et al., 1993; Nagayama et al., 1983).

In conclusion, all these results indicate that anamorsin coordinates one [2Fe-2S] cluster per protein molecule.

Anamorsin Is a Mia40 Substrate

Following the suggestion of our bioinformatic sequence analysis and the localization results of the yeast homolog (Zhang et al., 2008), we predict that anamorsin can be a putative substrate of Mia40 in the intermembrane space of mitochondria. Therefore, we have investigated the interaction of these two proteins in vitro.

The fully oxidized Mia40 containing three disulfide bonds ($Mia40_{3S\text{-}S}$) was incubated with anamorsin from which the Fe/S cluster was removed (apo-anamorsin) and that therefore has 10 free cysteines (two in the N-terminal folded domain and eight

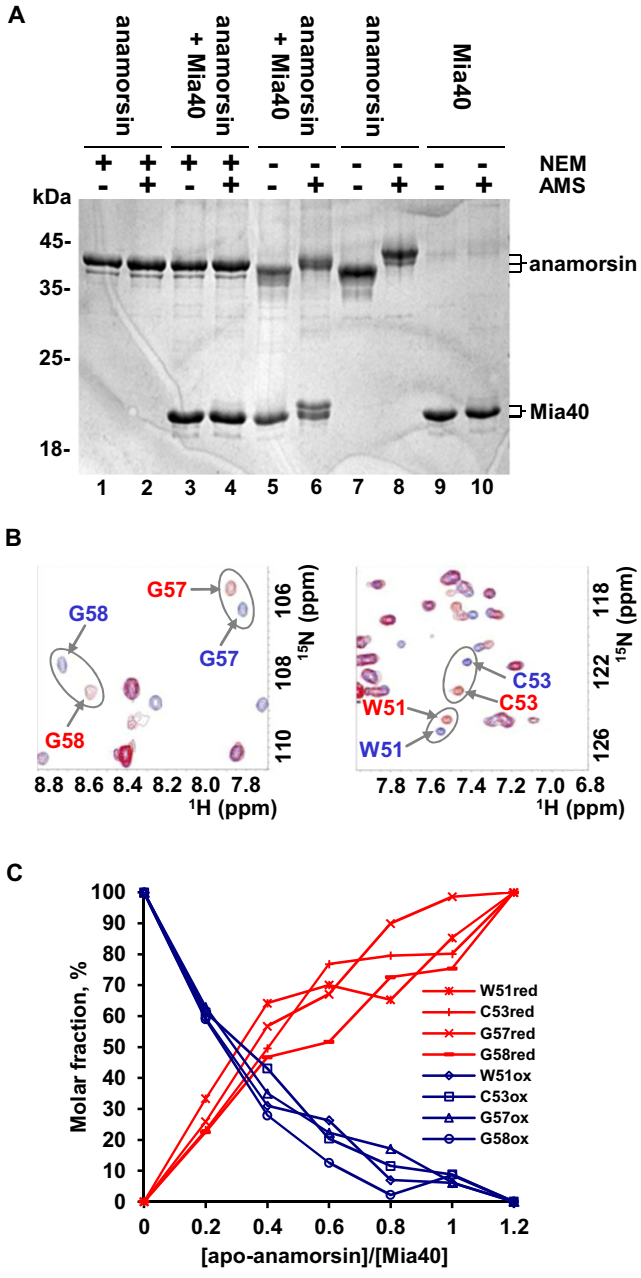

Figure 4. Interaction of Anamorsin with Mia40

(A) Seventeen percent SDS PAGE showing the redox state of apo-anamorsin and Mia40 alone or after their incubation in the presence (+) or absence (−) of the cysteine-alkylating agent AMS. After the incubation of the two proteins (lane 6) the band corresponding to Mia40 is shifted compared to the fully oxidized protein (lane 10) indicating a partial reduction of the protein. The shift of anamorsin band in lane 6 is not as strong as before incubation with Mia40 (lane 8) due to the oxidation of some of the cysteines of anamorsin. As a negative control, anamorsin was pretreated with NEM that blocks the cysteine residues (lanes 1–4).

(B) Overlay of two selected regions of the ^{1}H-^{15}N HSQC spectra of ^{15}N-labeled Mia40 in the presence of 0 (blue, $Mia40_{3S\text{-}S}$) and 1.2 equivalents (red, $Mia40_{2S\text{-}S}$) of unlabeled apo-anamorsin.

(C) The plot reports $Mia40_{3S\text{-}S}$/$Mia40_{2S\text{-}S}$ molar fraction as a function of the anmorsin/Mia40 molar ratio. The NH cross-peaks of residues Trp51, Cys53, Gly57, and Gly58 of Mia40, whose ^{1}H- and ^{15}N chemical shifts change substantially depending on the redox state of Mia40, have been selected to calculate the molar fraction (see also Figure S3).

in the CIAPIN1 domain). The analysis of the redox state of the two proteins after their incubation, performed by reaction with 4-acetamido-4′-maleimidylstilbene-2,2′-disulfonic acid (AMS) and followed by SDS-PAGE, showed that the band of Mia40 is upshifted with respect to the band of the fully oxidized $Mia40_{3S\text{-}S}$ before reaction (Figure 4A). This indicates that its cysteines were partially reduced on incubation with anamorsin and therefore, they bound two AMS molecules (0.5 kDa/thiol moiety). Anamorsin in the completely reduced state (before Mia40-incubation) binds 10 AMS molecules resulting in a larger gel-shift (Figure 4A). After incubation with $Mia40_{3S\text{-}S}$, this shift is decreased, indicating fewer AMS molecules bound to anamorsin as a consequence of the oxidation of some of its cysteine residues. As a negative control, anamorsin pretreated with N-ethylmaleimide (NEM) showed no gel-shift after reaction with Mia40, as no free cysteines are available for binding of AMS molecules (Figure 4A).

The redox process between apo-anamorsin and Mia40 was then followed by NMR. On addition of increasing amounts of unlabeled reduced apo-anamorsin to ^{15}N labeled $Mia40_{3S\text{-}S}$, NH chemical shift changes were detected in the ^{1}H-^{15}N HSQC spectra for Mia40 residues of the catalytic CPC motif and its surroundings, indicating its reduction ($Mia40_{2S\text{-}S}$, Figure 4B). The observed chemical shift variations are fully comparable with those due to the oxidation of typical IMS Mia40-substrates with twin CX_9C motifs (Banci et al., 2009). The reaction was complete at a Mia40/apo-anamorsin ratio of about 1:1 (Figure 4C). The same behavior was observed when the NMR experiment was performed using anamorsin carrying the Fe/S cluster ([2Fe-2S]-anamorsin hereafter). Moreover, the UV/vis and EPR spectra of [2Fe-2S]-anamorsin are similar before and after reaction with Mia40 (Figure S2). All these data indicate that the coordination of the cluster is not affected by the formation of the Mia40-induced disulfide bond(s).

When ^{15}N labeled [2Fe-2S]-anamorsin is added to unlabeled $Mia40_{3S\text{-}S}$, no significant chemical shift variations were observed in the ^{1}H-^{15}N HSQC maps for the residues of the folded N-terminal domain, indicating that it is not involved in the reaction (Figure S3). On the contrary, chemical shift variations are observed for NH signals in the crowded, central spectral region, indicating a structural rearrangement in the unstructured C-terminal region of anamorsin due to disulfide formation (Figure S3). Mia40-induced oxidation of anamorsin also produces a dramatically enhanced stability against protein degradation as shown by SDS-PAGE analysis of the protein mixture over time (Figure S3).

Carboxyamidomethylation with iodoacetamide (IAM) of the cysteine residues of [2Fe-2S]-anamorsin was performed before and after incubation with Mia40 to investigate how many cysteines and which ones are involved in the formation of the disulfide bond(s). After protein separation by SDS-PAGE and in-gel digestion with trypsin or chymotrypsin, the resulting peptide fragments were analyzed by matrix-assisted laser desorption/ionization mass spectrometry (MALDI-MS) (Supplemental Experimental Procedures). For anamorsin not treated with Mia40, all of the 10 cysteines reacted with IAM (Table S2),

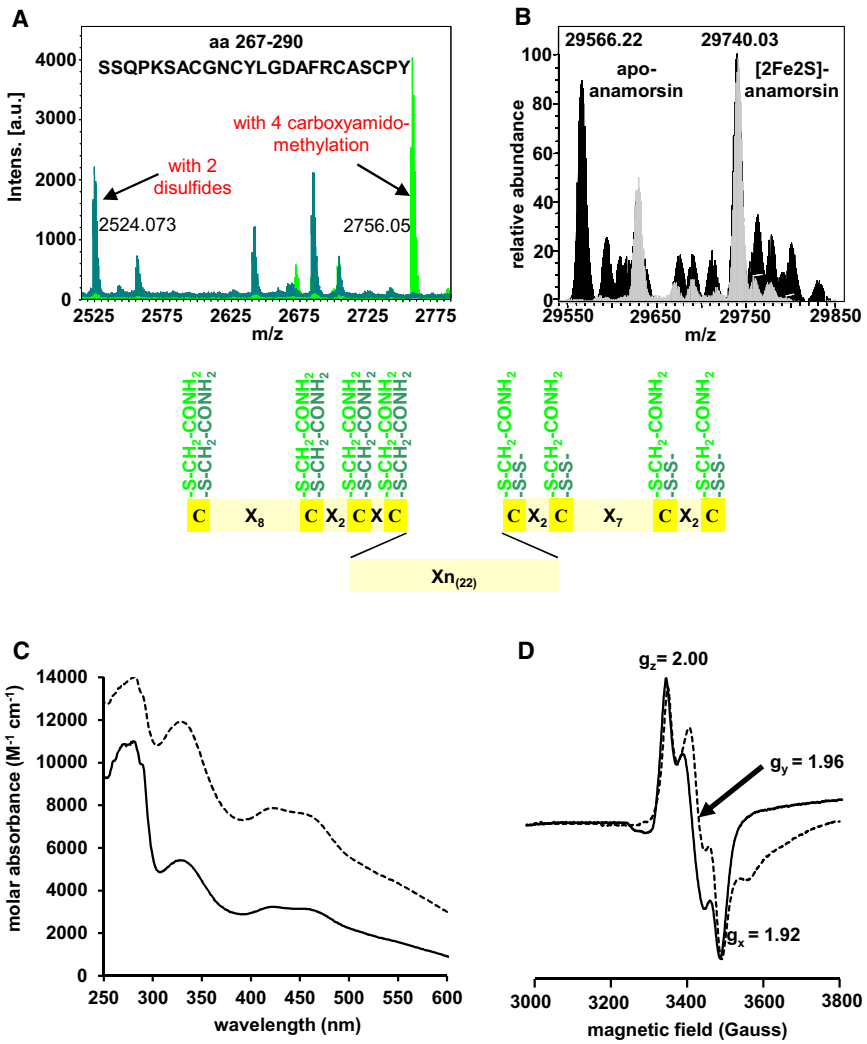

Figure 5. Identification of the Cysteines of Anamorsin Oxidized by Mia40 and Involved in [2Fe-2S] Cluster Coordination

(A) Overlay of matrix-assisted laser desorption/ionization mass spectrometry spectra of anamorsin before (light green) and after (dark green) reaction with Mia40. The cysteine residues were carboxyamidomethylated with IAM before proteins were subjected to SDS-PAGE and in-gel digested by chymotrypsin. Schematic representation of the alkylation pattern of the cysteine residues of the CIAPIN1 domain before (light green) and after (dark green) reaction with Mia40.

(B) Overlay of the electrospray ionization mass spectrometry spectra of C-terminally truncated [2Fe-2S]-anamorsin (gray shaded) and after addition of 0.025% formic acid (black). The C-terminally truncated apo form (MW 29566.22) was formed by acidification. The relative abundance was scaled with respect to the peak corresponding to the MW of C-terminally truncated [2Fe-2S]-anamorsin.

(C) UV-visible (50 mM Tris pH 8, 500 mM NaCl, 5% glycerol) and (D) EPR spectra at 45 K (50 mM Tris pH 8, 500 mM NaCl, 10% glycerol) of the C-terminally truncated (solid line) and full-length [2Fe-2S]-anamorsin (dashed line) (see also Table S2).

whereas in the sample incubated with Mia40 the last four cysteine residues (C274, C277, C285, and C288) did not react with IAM, and the remaining six cysteine residues were IAM-modified (Table S2 and Figure 5A). This means that the last four cysteine residues are involved in two disulfide bonds. Consequently, the other four upstream cysteines are coordinating the Fe/S cluster (C237, C246, C249, and C251), as the remaining two IAM-modified cysteines C92 and C116, located within the well-folded N-terminal domain, are not involved in Fe/S cluster binding according to the not-observed interaction between the N-terminal and CIAPIN1 domain (see second section of Results). To confirm this finding on the coordination mode of the [2Fe-2S] cluster, we produced a construct where the last four cysteine residues, those oxidized by Mia40, were removed (Supplemental Experimental Procedures). The UV/vis and EPR spectra of this construct showed the same features of the full-length anamorsin (Figures 5C and 5D), in agreement with the participation of the **C**X_8**C**X_2**C**X**C** motif in [2Fe-2S] cluster binding as determined by the MALDI-MS analysis. In this construct, the presence of a [2Fe-2S] cluster was also confirmed by electrospray ionization mass spectrometry (ESI-MS) analysis (Supplemental Experimental Procedures). The molecular weight difference between [2Fe-2S]-anamorsin and apo-anamorsin is 175.78 corresponding to the mass of 2Fe and 2S atoms (Figure 5B).

To test the specificity of Mia40/anamorsin recognition, the MALDI-MS approach used above was applied on apo-anamorsin that has, in contrast to the [2Fe-2S]-anamorsin, all cysteines available to react with Mia40. The resulting peptide fragments were the same as those in [2Fe-2S]-anamorsin after Mia40 incubation (Table S2). This shows that Mia40 specifically oxidizes only the C-terminal twin CX_2C motifs through the formation of two disulfide bonds. The specificity in the recognition of anamorsin by Mia40 was additionally assessed by incubating fully reduced apo-anamorsin with the fully oxidized human sulfhydryl oxidase ALR. The SDS-PAGE analysis of the AMS-reacted samples before and after incubation of the two proteins revealed no differences in the band pattern (Figure S3). Hence, ALR, in clear contrast to Mia40, cannot oxidize the cysteine residues of anamorsin.

To investigate the physiological relevance of the observed specific Mia40/anamorsin recognition, we tested (1), whether anamorsin can be imported in isolated mitochondria; and (2), the direct physical interaction between anamorsin and Mia40. To address these questions we produced anamorsin as a radioactive ^{35}S-labeled precursor in vitro in a reticulocyte lysate in vitro translation system. As can be seen in Figure 6A, anamorsin is imported in isolated mitochondria because it is protected against externally added trypsin (lane 2, Figure 6A) but becomes

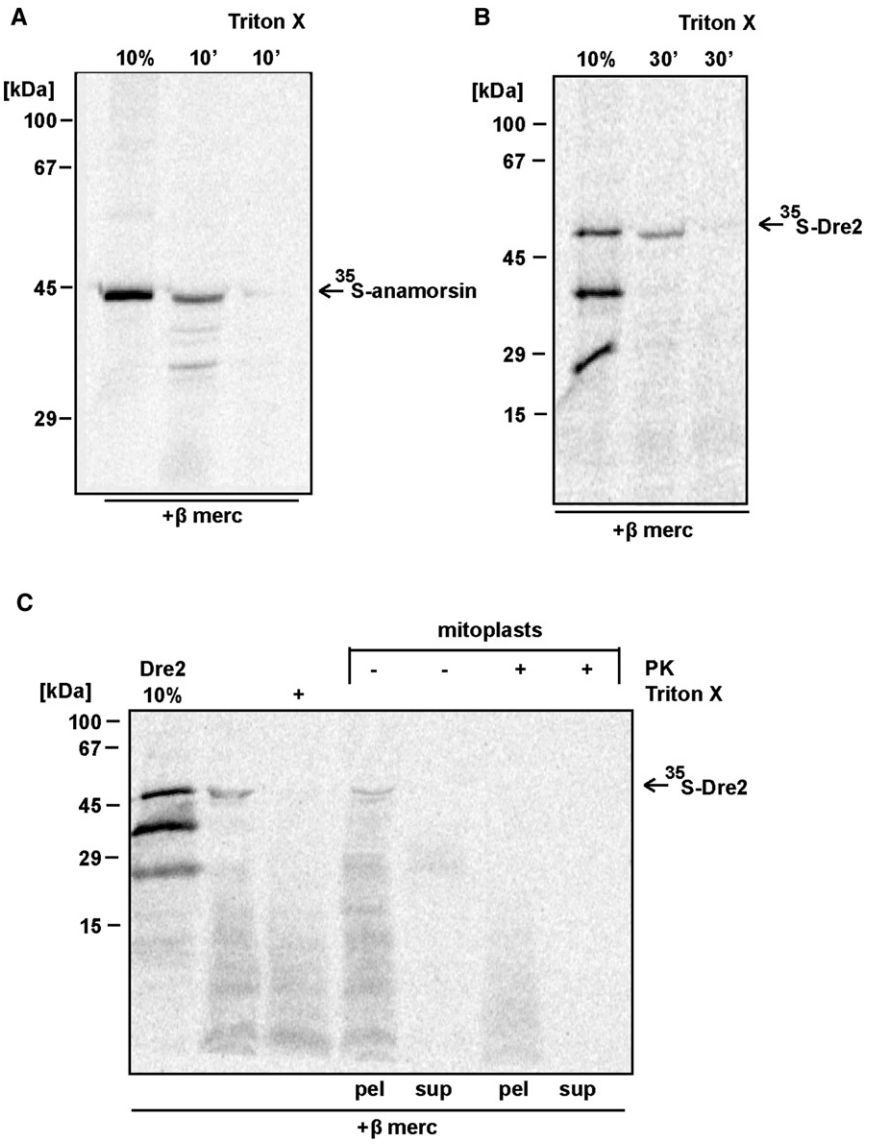

Figure 6. Import of Anamorsin and Dre2 into Mitochondria and Localization of Dre2 within Mitochondria

(A and B) Radiolabeled anamorsin (A) or Dre2 (B) was denatured with urea for 3 hr or 90 min at 37°C, respectively, and the import reactions were performed for the indicated time points at 30°C. Unimported material was removed by trypsin treatment and as a control for the import a sample treated with Triton X-100 was used. Samples were analyzed by SDS-PAGE (with β-mercaptoethanol in the sample buffer) and visualized by digital autoradiography.

(C) Import of radiolabeled Dre2 in wild-type mitochondria was performed for 5 min. For the specific mitochondrial localization of the imported Dre2, mitoplasting was performed and part of the mitoplasts was treated with Proteinase-K (PK). Matrix (pellet; pel) and the IMS (supernatant; sup) fractions were separated and analyzed (autoradiography) (see also Figure S4).

degraded on solubilization of the mitochondria with the detergent Triton X-100 (lane 3, Figure 6A). Because previous fractionation experiments of yeast cells had indicated that a small fraction of Dre2 was found in the IMS of mitochondria (Zhang et al., 2008), we tested directly for import of Dre2 in isolated mitochondria and we found that Dre2 is imported in the same manner as anamorsin (Figure 6B). Localization experiments after import of ^{35}S-Dre2 showed that the imported protein is in the IMS side of the mitochondrial inner membrane and not in the matrix, and becomes fully degraded by added trypsin on opening of the outer membrane by osmotic shock (mitoplasting, Figure 6C). Although the study by Zhang et al. (2008) had indicated that Dre2 is soluble in the IMS, we find that the imported protein is rather associated with the inner membrane. This association with the inner membrane may indicate association of imported Dre2 with a protein component of the inner membrane. A similar behavior has been observed before for other intrinsically soluble IMS proteins (for example the Tim10 protein) when they were used as radioactive precursors for import experiments (Luciano et al., 2001).

To test the direct physical interaction between Mia40 and anamorsin (or Dre2), we set up an assay where the mixed disulfide intermediate, predictable on the basis of the observed disulfide exchange reaction between Mia40 and anamorsin, was trapped (see Experimental Procedures). We see that yeast ΔN290Mia40 (a fully functional version of Mia40 missing the N-terminal 290 residues, responsible for its mitochondrial inner membrane anchoring (Banci et al., 2009; Sideris et al., 2009), thus making it completely soluble) interacted in a time-dependent manner with radiolabeled anamorsin (Figure 7A, lanes 3–6) to give a clearly identifiable covalent complex (indicated by an arrow), that is β-mercaptoethanol sensitive (Figure 7A, lane 8). When the SPS mutant of ΔN290Mia40 that is mutated in the active site cysteines (and that has been shown previously to lose its capacity to bind covalently to substrates (Banci et al., 2009)) was used in this assay no complex formation could be seen (Figure 7A, lane 7). This behavior is characteristic of the interaction between Mia40 and its substrates (Sideris and Tokatlidis, 2010), indicating that anamorsin physically interacts with Mia40. We further confirmed this result for the interaction of anamorsin with human Mia40 performing a similar in vitro assay (Figure 7B) as well as for the interaction between yeast Dre2 and yeast Mia40.

The import results together with the direct binding of Mia40 to Dre2/anamorsin suggested that such an interaction should exist in mitochondria. To address this point, we performed the following experiment: radioactive Dre2 was incubated with yeast mitochondria during an osmotic shock that ruptures selectively the outer membrane (mitoplasting); in these conditions

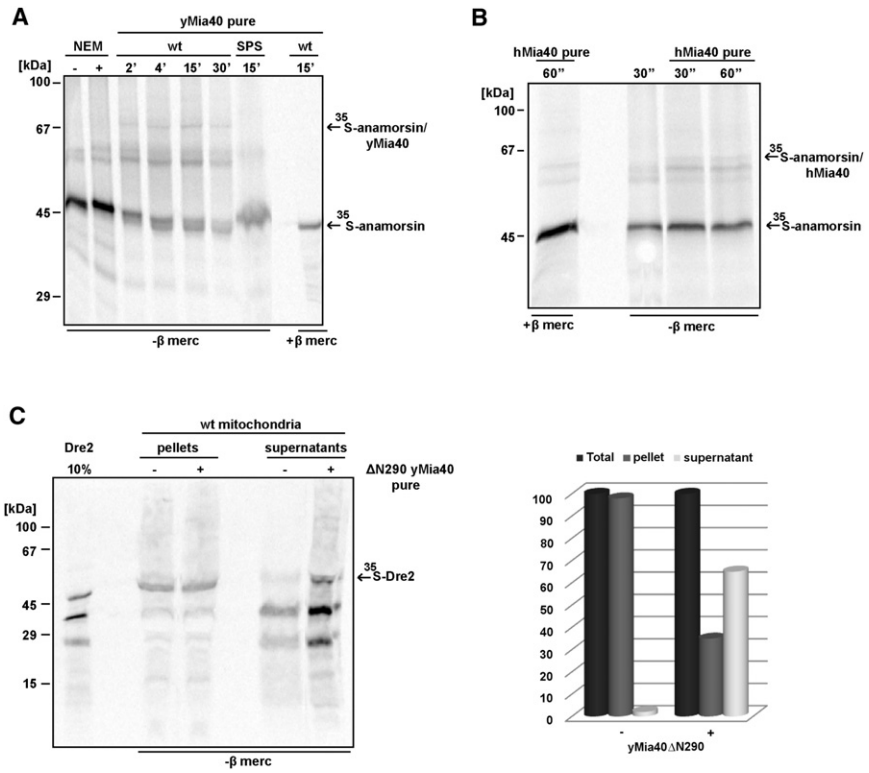

Figure 7. Physical Interaction of Anamorsin with Mia40 and Competition Assay

(A and B) Radiolabeled, denatured anamorsin was incubated with pure ΔN290 yeast Mia40 (yMia40) wt (A) or SPS mutant (A) or with human Mia40 (hMia40) (B). The reactions were terminated by trichloroacetic acid precipitation at the indicated time points. Samples were analyzed by SDS-PAGE and visualized by digital autoradiography.

(C) Radiolabeled Dre2 was incubated with wild-type mitochondria for 30 min while mitoplasting at 4°C. For competition against the endogenous Mia40, pure ΔN290 yeast Mia40 was added to the reaction in a 1:1 ratio. Reactions were blocked with 25 mM NEM before the separation of the matrix (pellet; pel) and the IMS (supernatant; sup) (autoradiography). Quantification of Dre2 after mitoplasing with and without addition of pure ΔN290 yeast Mia40 in both pellets and supernatants (see also Figure S4).

radioactive Dre2 interacts with the endogenous Mia40 that is anchored to the inner membrane through its N-terminal transmembrane helix and hence Dre2 was found associated to the membrane pellet (Figure 7C, lanes 2 and 3). In the IMS supernatant fraction only a minor proportion of Dre2 was present (Figure 7C, lane 4), in agreement with the localization experiment shown in Figure 6C. However, when the mitoplasting was done in the presence of soluble ΔN290Mia40, the amount of Dre2 in the supernatant was substantially increased (Figure 7C, lane 5). The most likely explanation for this is that the soluble ΔN290Mia40 added during mitoplasting competed efficiently the binding of Dre2 by endogenous Mia40 anchored in the inner membrane, thereby "segregating" most of radioactive Dre2 into the supernatant fraction. This result points to the conclusion that the observed interactions between Dre2 (and anamorsin) and Mia40 are physiological.

DISCUSSION

Anamorsin is formed by a SAM-dependent methyltransferase-like structural domain, but with no cofactor SAM binding properties, and a C-terminal CIAPIN1 domain. These two domains are connected by an unstructured and flexible linker. The CIAPIN1 domain contains a highly conserved cysteine pattern and is found in several eukaryotic proteins (with members ranging from basal protozoa to fungi, higher plants and animals, up to humans). The highly conserved cysteine pattern of the CIAPIN1 domain is involved in the binding of a [2Fe-2S] cluster exploiting the first four cysteines of the pattern, i.e., $\mathbf{C}X_{5\text{-}14}\mathbf{C}X_2\mathbf{C}X\mathbf{C}$, thus defining a novel cysteine-binding motif for Fe/S proteins. We show this by an extensive characterization combining NMR, UV/vis, EPR, and both ESI-MS and MALDI-MS techniques. Yeast Dre2 has been proposed to bind a [4Fe-4S] cluster in addition to the [2Fe-2S] cluster, but only on the basis of EPR data, which, as also mentioned by the authors, need further detailed investigation to be fully interpreted (Zhang et al., 2008). The [2Fe-2S] cluster in anamorsin is located in a flexible C-terminal region and this property is reminiscent of proteins involved in Fe/S cluster biogenesis, like the ISU-type proteins (Bertini et al., 2003; Kim et al., 2009; Mansy et al., 2004) and the NFU protein (Liu and Cowan, 2009). The observed structural flexibility of the Fe/S cluster containing region can be relevant for the interaction with diverse partner proteins in different cellular compartments.

It is being increasingly recognized that the IMS plays a pivotal role in the coordination of mitochondrial activities with other cellular processes (Herrmann and Riemer, 2010). Proteins of the IMS are particularly relevant for the coordinated exchange of components/signals into and out of mitochondria. One of these processes is represented by the connection between the mitochondrial-matrix localized Fe/S protein biogenesis machinery to that of the cytosol; still not all of the key proteins relevant to these two pathways are known. Up to now, only one component, an ABC membrane transporter of the mitochondrial inner membrane, is found to be involved in exporting from the matrix to the IMS a yet unidentified product of the ISC assembly pathway that is essential for the cytosolic Fe/S protein production (Cavadini et al., 2007; Kispal et al., 1999; Kuhnke et al., 2006). This export reaction is further facilitated in the IMS by the sulfhydryl oxidase Erv1/ALR and glutathione (Lange et al., 2001; Lill and Mühlenhoff, 2006). On the basis of its protein IMS localization, the yeast homolog of anamorsin, Dre2, has been proposed to play a functional role in the assembly process of cytosolic Fe/S clusters once imported in the IMS, i.e., to generate a component or signal that is permissive for the subsequent assembly steps in the cytoplasm (Zhang et al., 2008). In addition, it has recently been suggested that Dre2 in the cytosol

can receive electrons from the diflavin reductase Tah18 to act as an electron donor necessary for Fe/S cluster incorporation into cytosolic CIA proteins (Netz et al., 2010). The proposed cytosolic electron transfer between Dre2 and Tah18 was found to be conserved in humans as the human homologs, anamorsin and Ndor1, can functionally replace their yeast counterparts and interact with each other (Netz et al., 2010).

Our data show that anamorsin interacts with the well-known mitochondrial oxidoreductase Mia40. In particular, Mia40 is able to specifically catalyze the formation of two disulfide bonds that involve the four cysteines of the twin CX_2C motif. The latter is indeed not involved in iron-binding and is located downstream of the cysteines involved in Fe/S cluster-binding. Mitochondrial proteins can be directed to the IMS by internal cysteine-containing targeting signals that allow passage through the import TOM translocase (Riemer et al., 2011; Sideris et al., 2009). The cysteine residues in these signals (usually CX_3C, CX_9C motifs but also CX_2C motifs) are recognized by the IMS-localized oxidoreductase Mia40 that serves as an intramitochondrial import receptor and traps substrate proteins within this compartment by forming disulfides (Banci et al., 2010; Riemer et al., 2011). Our data suggests that anamorsin could, in this way, be transported into and retained in the IMS. Consistent with this proposal we have found that: (1), both anamorsin and Dre2 are imported efficiently into isolated mitochondria; (2), the CIAPIN1 domain in its fully reduced apo-state is completely unfolded, which is a typical structural feature of the recognition sites of Mia40-substrates; (3), both anamorsin and Dre2 interact physically with Mia40 in vitro and Dre2 also in organello; and (5), Mia40 specifically oxidizes the twin CX_2C motif of anamorsin without interfering with the Fe/S cluster binding. These findings suggest that anamorsin/Dre2 can acquire the [2Fe-2S] cluster, to work as electron transfer protein, also once trapped by Mia40 in the IMS. The latter concept has been found in the mitochondrial copper chaperone Cox17, which is involved in the assembly of the copper centers of cytochrome *c* oxidase once imported in the IMS (Robinson and Winge, 2010). Cox17, similarly to anamorsin, undergoes Mia40-induced formation of two disulfide bonds between a twin CX_9C motif, whereas two additional cysteines, involved in copper binding and positioned upstream of the twin CX_9C motif, similarly to the Cys motif of anamorsin involved in Fe/S cluster-binding, are not oxidized by Mia40, thus being capable to coordinate the copper(I) ion (Banci et al., 2008). The fact that the cluster assembly in Dre2/anamorsin is independent of the cytosolic CIA components (Netz et al., 2010) is also in agreement with a cluster maturation of Dre2/anamorsin being operative not only in the cytoplasm but also in other compartments such as the IMS. The fact that the IMS-localized Mia40 protein partner Erv1 is specifically required for the maturation of cytosolic Fe/S proteins (Lange et al., 2001) and that Dre2/anamorsin is trapped by the Mia40/Erv1 IMS-machinery can be an explanation for the requirement of Erv1 in the assembly of the cytosolic Fe/S cluster proteins. Therefore, anamorsin links the Mia40/Erv1-dependent IMS protein trapping machinery to the cytosolic Fe/S maturation process.

All the above considerations suggest that anamorsin can play a functional role in the cytosolic Fe/S cluster maturation process not only in the cytoplasm as recently reported (Netz et al., 2010), but also in the IMS once trapped there through the Mia40-Erv1 pathway, thus potentially being a member of the ISC export machinery. A similar double functionality in different cellular compartments has been found for other IMS proteins such as the superoxide dismutase and its copper chaperone CCS that, similarly to anamorsin, have both cytosolic and IMS localization playing the same function in both compartments and being trapped in the IMS through the Mia40/Erv1 machinery (Culotta et al., 2006; Kawamata and Manfredi, 2010). We can, however, not exclude that anamorsin/Dre2 can perform another function when localized in the IMS. Indeed, it has been reported that Dre2 cytosolic protein partner Tah18 relocalizes to mitochondria on oxidative stress to induce cell apoptosis, and anamorsin is linked to apoptosis-related processes (Shibayama et al., 2004; Vernis et al., 2009). Therefore, the IMS-localized anamorsin/Dre2 could also be part of the cell death program.

SIGNIFICANCE

The human protein anamorsin was implicated in cytosolic Fe/S cluster assembly, but no molecular background information for this protein is still available. In this work, the structural-dynamical characterization of anamorsin has been reported for the first time. The protein contains two structurally independent domains connected by an unstructured, 50 amino acid-long linker. The C-terminal domain binds a [2Fe-2S] cluster through a previously unknown cysteine binding motif in Fe/S proteins and specifically interacts with Mia40, an oxidoreductase typically involved in protein trapping in the mitochondrial intermembrane space (IMS). Mia40 catalyzes downstream of the Fe/S binding site the formation of two disulfide bonds in a twin CX_2C motif of the C-terminal domain of anamorsin. The fact that anamorsin is imported in the IMS together with the detection of an intermolecular disulfide-bonded intermediate between Mia40 and anamorsin suggest that their interaction should exist in mitochondria. Our findings suggest a possible functional role of anamorsin in the cytosolic Fe/S cluster biogenesis, once imported in the IMS, and they will have a general impact on the community studying the Fe/S cluster biogenesis.

EXPERIMENTAL PROCEDURES

UV/Vis, EPR, and NMR Spectroscopy

UV/vis spectra of oxidized and reduced [2Fe-2S]-anamorsin in degassed 50 mM phosphate buffer at pH 7.0 were performed on a Cary 50 Eclipse spectrophotometer.

EPR spectra of oxidized and reduced [2Fe-2S]-anamorsin in 50 mM Tris-HCl pH 8.0, 500 mM NaCl, or 50 mM phosphate buffer at pH 7.0 and 10% glycerol was performed on a Bruker Elexsys E500 spectrometer equipped with a X-band microwave bridge (microwave frequency, 9.45 GHz) and an unit for temperature control (ER 4131 VT). EPR parameters were: sample temperature 45 K; microwave frequency 9.45 GHz; microwave power 5 mW; modulation frequency 9,387,691 GHz; modulation amplitude 2500 G, time constant 167 ms. To reduce the cluster, 1–10 mM dithionite was added under anaerobic conditions and the sample was immediately frozen.

^1H paramagnetic NMR spectra of 2 mM oxidized [2Fe-2S]-anamorsin (50 mM phosphate buffer pH 7.0 in D_2O, 1 mM DTT) were recorded on a Bruker Avance 600 MHz spectrometer equipped with a selective ^1H probe head (5 mm SEL ^1H) at 298 K. All 1D spectra were taken by using a super WEFT pulse sequence (Inubushi and Becker, 1983) with a recycle delay of 54 ms.

All NMR spectra to obtain the solution structure of the N-terminal domain of anamorsin (aa 1–172) were recorded at 298 K using Bruker Avance 500, 600,

and 900 MHz spectrometers, processed using the standard Bruker software Topspin and analyzed by the program CARA (Keller, 2004). The NMR experiments used for resonance assignment and structure calculations were performed on ^{13}C-/^{15}N-labeled or on ^{15}N-labeled samples (0.5–1 mM) in 50 mM phosphate buffer pH 7, 2 mM DTT containing 10% (v/v) D_2O. The ^{1}H, ^{13}C, and ^{15}N backbone resonance assignment was performed using standard triple-resonance NMR experiments and side chain assignment using TOCSY- and NOESY-based NMR experiments.

Interaction of Anamorsin with Mia40

$Mia40_{3S-S}$ was incubated with fully reduced apo-anamorsin for 5 min at room temperature before analysis of cysteine redox states of the mixture with AMS and SDS-PAGE as described in Banci et al. (2009). To check the specificity of anamorsin and Mia40 interaction, the same procedure was performed with fully reduced apo-anamorsin and the short (cytosolic) or long (IMS) isoform of human ALR in a fully oxidized state.

To monitor the interaction by NMR, titrations of ^{15}N-labeled apo- or [2Fe-2S]-anamorsin with unlabeled $Mia40_{3S-S}$ and of unlabeled apo- or [2Fe-2S]-anamorsin with ^{15}N-labeled $Mia40_{3S-S}$ were performed at 298 K. Chemical shift changes were followed by ^{1}H-^{15}N HSQC spectra after addition of increasing amounts of the unlabeled partner.

To detect the location of the Mia40-induced disulfides in the anamorsin sequence, a full-length [2Fe-2S]-anamorsin or apo-anamorsin sample was divided into two aliquots I and II (50 μl each). Sample II was mixed with 12.5 μl of 700 μM $Mia40_{3S-S}$ and incubated at room temperature for 5 min. Both samples were then precipitated with 20% trichloroacetic acid (TCA), subsequently washed with acetone and resuspended in 50 μl of degassed buffer (Tris-HCl 50 mM, Urea 8 M pH 7.5). Ten microliters of freshly prepared 100 mM IAM were added to each sample and the mixture was incubated in anaerobic conditions at 25°C in the dark for 1 hr. Reacted samples were applied on a SDS-PA gel and run without DTT. Bands corresponding to anamorsin from both sample I and II were excised from the gel and individually transferred to a 1.5 ml microcentrifuge tube. These gel pieces were proteolytically digested and the resulting peptide fragments analyzed by MALDI-MS (Supplemental Experimental Procedures).

Protein Import and Localization in Yeast Mitochondria

^{35}S-labeled precursor proteins (Dre2 and anamorsin) were synthesized using the TNT SP6-coupled transcription/translation kit (Promega). The radioactive material was incubated with ammonium sulfate (67% saturated solution) for 30 min on ice, followed by centrifugation at 25,000 × g, for 30 min at 4°C. The obtained pellet was resuspended in 8 M urea, 10 mM EDTA, 50 mM HEPES pH 7.4, and 5 mM β-mercaptoethanol (anamorsin, Dre2) or 10 mM DTT (Dre2). Anamorsin was denatured for 3 hr and Dre2 for 90 min or 3 hr, both at 37°C. The denatured radioactive precursors were incubated with 50 μg of wild-type yeast mitochondria in the presence of 2 mM ATP and 2.5 mM NADH for the indicated time points at 30°C. Mitochondria were resuspended in 1.2 M sorbitol and 20 mM HEPES, pH 7.4, followed by a treatment with 0.05 mg/ml trypsin (30 min on ice) to remove unimported material, followed by inactivation of the protease with 0.5 mg/ml soybean trypsin inhibitor.

In the localization experiments, the above import procedure was followed by the production of mitoplasts (mitochondria with their outer membrane broken). These were produced by osmotically shocking 250 μg mitochondria, resuspending them in 1× import buffer (Sideris and Tokatlidis, 2010) at 5 mg/ml and diluting them 10 times in the hypotonic buffer 20 mM HEPES, pH 7.4, for 30 min on ice. To the mitoplasted mitochondria proteinase K (PK) was added for proteolytic digestion. Pellet and supernatant fractions were separated by centrifugation. As a control of the mitoplasting process, antibodies against the known mitochondrial marker protein Cpn10 (Cpn10: Chaperonin 10) were used (immunoblot) (Figure S4).

All samples were resuspended in Laemmli sample buffer with β-mercaptoethanol, analyzed by SDS-PAGE, and visualized by digital autoradiography (Molecular Dynamics).

In Vitro Binding Assays

^{35}S-labeled precursor proteins (anamorsin and Dre2) were synthesized and denatured as mentioned above. Two microliters of denatured precursor was incubated on ice for the indicated time points using pure yeast (wt and SPS mutant) or human Mia40 at 2.5 mg/ml. The reactions were terminated by TCA precipitation (10%). Samples were resuspended in Laemmli sample buffer with and without β-mercaptoethanol and containing 10 mM NEM, analyzed by SDS-PAGE, and visualized by digital autoradiography (Molecular Dynamics).

Competition Assay

The radiolabeled precursor was added while mitoplasting yeast mitochondria. Pure yeast ΔN290 Mia40 was then added in an estimated 1:1 ratio, taking into consideration the endogenous amount of Mia40. Reactions were blocked with 25 mM NEM addition. After centrifugation, the supernatant (representing the IMS) was precipitated by 10% TCA. Finally, samples (pellets and supernatants) were resuspended in Laemmli sample buffer without β-mercaptoethanol, analyzed by SDS-PAGE, and visualized by digital autoradiography (Molecular Dynamics). Mitoplasting was confirmed with immunodecoration against known mitochondrial marker proteins (Cytb2: Cytochrome b2 that is IMS-localized, and cpn10: chaperonin 10 that is matrix-localized) (Figure S4). For quantification of the amount of Dre2 in the supernatant and pellet fractions, the program Image Quant 5.2 was used to make standard curves and estimate the intensities of the radioactive bands.

ACCESSION NUMBERS

The atomic coordinates, structural restraints, and resonance assignments of the N-terminal domain of anamorsin (1-172) have been deposited in the Protein Data Bank (PDB ID: 2ld4) and BioMagResBank (BMRB Accession Code: 17646), respectively.

SUPPLEMENTAL INFORMATION

Supplemental Information includes Supplemental Experimental Procedures, four figures, and two tables and can be found with this article online at doi:10.1016/j.chembiol.2011.03.015.

ACKNOWLEDGMENTS

This work was supported by EU-SFMET contract no. 201640, by EU Bio-NMR contract no. 261863, and by the Italian MIUR-FIRB PROTEOMICA-RBRN07BMCT (to I.B. and L.B.) and funds from IMBB-FORTH, the University of Crete, and the European Social Fund and national resources (to K.T.). Manuele Migliardi (CERM, University of Florence) is acknowledged for performing EPR measurements and Nitsa Katrakili and Babis Pozidis (IMBB-FORTH) for excellent technical assistance.

Received: October 12, 2010
Revised: February 24, 2011
Accepted: March 8, 2011
Published: June 23, 2011

REFERENCES

Andreini, C., Banci, L., Bertini, I., Elmi, S., and Rosato, A. (2007). Non-heme iron through the three domains of life. Proteins *67*, 317–324.

Andreini, C., Bertini, I., Cavallaro, G., Najmanovich, R.J., and Thornton, J.M. (2009). Structural analysis of metal sites in proteins: non-heme iron sites as a case study. J. Mol. Biol. *388*, 356–380.

Banci, L., Bertini, I., and Luchinat, C. (1990). The ^{1}H NMR parameters of magnetically coupled dimers—the Fe_2S_2 proteins as an example. Struct. Bond. *72*, 113–135.

Banci, L., Bertini, I., Ciofi-Baffoni, S., Janicka, A., Martinelli, M., Kozlowski, H., and Palumaa, P. (2008). A structural-dynamical characterization of human Cox17. J. Biol. Chem. *283*, 7912–7920.

Banci, L., Bertini, I., Cefaro, C., Ciofi-Baffoni, S., Gallo, A., Martinelli, M., Sideris, D.P., Katrakili, N., and Tokatlidis, K. (2009). MIA40 is an oxidoreductase that catalyzes oxidative protein folding in mitochondria. Nat. Struct. Mol. Biol. *16*, 198–206.

Banci, L., Bertini, I., Cefaro, C., Cenacchi, L., Ciofi-Baffoni, S., Felli, I.C., Gallo, A., Gonnelli, L., Luchinat, E., Sideris, D., et al. (2010). Molecular chaperone

function of Mia40 triggers consecutive induced folding steps of the substrate in mitochondrial protein import. Proc. Natl. Acad. Sci. USA *107*, 20190–20195.

Bertini, I., Turano, P., and Vila, A.J. (1993). Nuclear magnetic resonance of paramagnetic metalloproteins. Chem. Rev. *93*, 2833–2932.

Bertini, I., Ciurli, S., and Luchinat, C. (1995). The electronic structure of FeS centers in proteins and models. A contribution to the understanding of their electron transfer properties. Struct. Bond. *83*, 1–53.

Bertini, I., Luchinat, C., Provenzani, A., Rosato, A., and Vasos, P.R. (2002). Browsing gene banks for Fe2S2 ferredoxins and structural modeling of 88 plant-type sequences: an analysis of fold and function. Proteins *46*, 110–127.

Bertini, I., Cowan, J.A., Del Bianco, C., Luchinat, C., and Mansy, S.S. (2003). Thermotoga maritima IscU. Structural characterization and dynamics of a new class of metallochaperone. J. Mol. Biol. *331*, 907–924.

Cavadini, P., Biasiotto, G., Poli, M., Levi, S., Verardi, R., Zanella, I., Derosas, M., Ingrassia, R., Corrado, M., and Arosio, P. (2007). RNA silencing of the mitochondrial ABCB7 transporter in HeLa cells causes an iron-deficient phenotype with mitochondrial iron overload. Blood *109*, 3552–3559.

Culotta, V.C., Yang, M., and O'Halloran, T.V. (2006). Activation of superoxide dismutases: putting the metal to the pedal. Biochim. Biophys. Acta *1763*, 747–758.

Gabriel, K., Milenkovic, D., Chacinska, A., Muller, J., Guiard, B., Pfanner, N., and Meisinger, C. (2007). Novel mitochondrial intermembrane space proteins as substrates of the MIA import pathway. J. Mol. Biol. *365*, 612–620.

Hao, Z., Li, X., Qiao, T., Zhang, J., Shao, X., and Fan, D. (2006a). Distribution of CIAPIN1 in normal fetal and adult human tissues. J. Histochem. Cytochem. *54*, 417–426.

Herrmann, J.M., and Riemer, J. (2010). The intermembrane space of mitochondria. Antioxid. Redox Signal. *13*, 1341–1358.

Inubushi, T., and Becker, E.D. (1983). Efficient detection of paramagnetically shifted NMR resonances by optimizing the WEFT pulse sequence. J. Magn. Reson. *51*, 128–133.

Kagan, R.M., and Clarke, S. (1994). Widespread occurrence of three sequence motifs in diverse S-adenosylmethionine-dependent methyltransferases suggests a common structure for these enzymes. Arch. Biochem. Biophys. *310*, 417–427.

Kawamata, H., and Manfredi, G. (2010). Import, maturation, and function of SOD1 and its copper chaperone CCS in the mitochondrial intermembrane space. Antioxid. Redox Signal. *13*, 1375–1384.

Keller, R. (2004). The Computer Aided Resonance Assignment Tutorial (CANTINA Verlag Goldau).

Kim, J.H., Fuzery, A.K., Tonelli, M., Ta, D.T., Westler, W.M., Vickery, L.E., and Markley, J.L. (2009). Structure and dynamics of the iron-sulfur cluster assembly scaffold protein IscU and its interaction with the cochaperone HscB. Biochemistry *48*, 6062–6071.

Kispal, G., Csere, P., Prohl, C., and Lill, R. (1999). The mitochondrial proteins Atm1p and Nfs1p are essential for biogenesis of cytosolic Fe/S proteins. EMBO J. *18*, 3981–3989.

Kuhnke, G., Neumann, K., Mühlenhoff, U., and Lill, R. (2006). Stimulation of the ATPase activity of the yeast mitochondrial ABC transporter Atm1p by thiol compounds. Mol. Membr. Biol. *23*, 173–184.

Lange, H., Lisowsky, T., Gerber, J., Mühlenhoff, U., Kispal, G., and Lill, R. (2001). An essential function of the mitochondrial sulfhydryl oxidase Erv1p/ALR in the maturation of cytosolic Fe/S proteins. EMBO Rep. *2*, 715–720.

Li, X., Wu, K., and Fan, D. (2010). CIAPIN1 as a therapeutic target in cancer. Expert Opin. Ther. Targets *14*, 603–610.

Lill, R. (2009). Function and biogenesis of iron-sulphur proteins. Nature *460*, 831–838.

Lill, R., and Mühlenhoff, U. (2006). Iron-sulfur protein biogenesis in eukaryotes: components and mechanisms. Annu. Rev. Cell Dev. Biol. *22*, 457–486.

Lill, R., and Mühlenhoff, U. (2008). Maturation of iron-sulfur proteins in eukaryotes: mechanisms, connected processes, and diseases. Annu. Rev. Biochem. *77*, 669–700.

Liu, Y., and Cowan, J.A. (2009). Iron-sulfur cluster biosynthesis: characterization of a molten globule domain in human NFU. Biochemistry *48*, 7512–7518.

Luciano, P., Vial, S., Vergnolle, M.A., Dyall, S.D., Robinson, D.R., and Tokatlidis, K. (2001). Functional reconstitution of the import of the yeast ADP/ATP carrier mediated by the TIM10 complex. EMBO J. *20*, 4099–4106.

Mansy, S.S., Wu, S.P., and Cowan, J.A. (2004). Iron-sulfur cluster biosynthesis: biochemical characterization of the conformational dynamics of Thermotoga maritima IscU and the relevance for cellular cluster assembly. J. Biol. Chem. *279*, 10469–10475.

Martin, J.L., and McMillan, F.M. (2002). SAM (dependent) I AM: the S-adenosylmethionine-dependent methyltransferase fold. Curr. Opin. Struct. Biol. *12*, 783–793.

Morimoto, K., Nishio, K., and Nakai, M. (2002). Identification of a novel prokaryotic HEAT-repeats-containing protein which interacts with a cyanobacterial IscA homolog. FEBS Lett. *519*, 123–127.

Nagayama, K., Ozaki, Y., Kyogoku, Y., Hase, T., and Matsubara, H. (1983). Classification of iron-sulfur cores in ferredoxins by ^{1}H nuclear magnetic resonance spectroscopy. J. Biochem. *94*, 893–902.

Netz, D.J., Stumpfig, M., Dore, C., Mühlenhoff, U., Pierik, A.J., and Lill, R. (2010). Tah18 transfers electrons to Dre2 in cytosolic iron-sulfur protein biogenesis. Nat. Chem. Biol. *6*, 758–765.

Palmer, G., and Sands, R.H. (1966). On the magnetic resonance of spinach ferredoxin. J. Biol. Chem. *241*, 253.

Prilusky, J., Felder, C.E., Zeev-Ben-Mordehai, T., Rydberg, E.H., Man, O., Beckmann, J.S., Silman, I., and Sussman, J.L. (2005). FoldIndex: a simple tool to predict whether a given protein sequence is intrinsically unfolded. Bioinformatics *21*, 3435–3438.

Riemer, J., Fischer, M., and Herrmann, J.M. (2011). Oxidation-driven protein import into mitochondria: Insights and blind spots. Biochim. Biophys. Acta. *1808*, 981–989.

Robinson, N.J., and Winge, D.R. (2010). Copper metallochaperones. Annu. Rev. Biochem. *79*, 537–562.

Rouault, T.A., and Tong, W.H. (2005). Iron-sulphur cluster biogenesis and mitochondrial iron homeostasis. Nat. Rev. Mol. Cell Biol. *6*, 345–351.

Schluckebier, G., O'Gara, M., Saenger, W., and Cheng, X. (1995). Universal catalytic domain structure of AdoMet-dependent methyltransferases. J. Mol. Biol. *247*, 16–20.

Schuster-Böckler, B., Schultz, J., and Rahmann, S. (2004). HMM Logos for visualization of protein families. BMC Bioinformatics *5*, 7.

Shibayama, H., Takai, E., Matsumura, I., Kouno, M., Morii, E., Kitamura, Y., Takeda, J., and Kanakura, Y. (2004). Identification of a cytokine-induced antiapoptotic molecule anamorsin essential for definitive hematopoiesis. J. Exp. Med. *199*, 581–592.

Sideris, D.P., and Tokatlidis, K. (2010). Trapping oxidative folding intermediates during translocation to the intermembrane space of mitochondria: in vivo and in vitro studies. Methods Mol. Biol. *619*, 411–423.

Sideris, D.P., Petrakis, N., Katrakili, N., Mikropoulou, D., Gallo, A., Ciofi-Baffoni, S., Banci, L., Bertini, I., and Tokatlidis, K. (2009). A novel intermembrane space-targeting signal docks cysteines onto Mia40 during mitochondrial oxidative folding. J. Cell Biol. *187*, 1007–1022.

Tong, W.H., and Rouault, T.A. (2006). Functions of mitochondrial ISCU and cytosolic ISCU in mammalian iron-sulfur cluster biogenesis and iron homeostasis. Cell Metab. *3*, 199–210.

Tong, W.H., Jameson, G.N., Huynh, B.H., and Rouault, T.A. (2003). Subcellular compartmentalization of human Nfu, an iron-sulfur cluster scaffold protein, and its ability to assemble a [4Fe-4S] cluster. Proc. Natl. Acad. Sci. USA *100*, 9762–9767.

Vernis, L., Facca, C., Delagoutte, E., Soler, N., Chanet, R., Guiard, B., Faye, G., and Baldacci, G. (2009). A newly identified essential complex, Dre2-Tah18, controls mitochondria integrity and cell death after oxidative stress in yeast. PLoS ONE *4*, e4376.

Zhang, Y., Lyver, E.R., Nakamaru-Ogiso, E., Yoon, H., Amutha, B., Lee, D.W., Bi, E., Ohnishi, T., Daldal, F., Pain, D.,, et al. (2008). Dre2, a conserved eukaryotic Fe/S cluster protein, functions in cytosolic Fe/S protein biogenesis. Mol. Cell. Biol. *28*, 5569–5582.